



High-throughput assay using a GFP-expressing replicon for SARS-CoV drug discovery

Feng Ge^{a,*}, Sheng Xiong^{a,1}, Fu-Sen Lin^b, Zhi-Ping Zhang^c, Xian-En Zhang^c

^a Institute of Life and Health Engineering, Jinan University, Guangzhou, Guangdong 510632, PR China

^b Division of Research, Singapore General Hospital, Singapore Health Research Facilities, 7 Hospital Drive, Block A, #02-05, Singapore 169611, Republic of Singapore

^c State Key Laboratory of Virology, Wuhan Institute of Virology, Chinese Academy of Sciences, Wuhan 430071, PR China

ARTICLE INFO

Article history:

Received 5 February 2008

Accepted 13 May 2008

Keywords:

SARS-CoV replicon

High-throughput screen (HTS)

ABSTRACT

The causative agent of severe acute respiratory syndrome (SARS) has been identified as a novel coronavirus, SARS-CoV. The development of rapid screening assays is essential for antiviral drug discovery. By using a cell line expressing a SARS-CoV subgenomic replicon, we developed a high-throughput assay and used it to screen small molecule compounds for inhibitors of SARS-CoV replication in the absence of live virus. The assay system involves minimal manipulation after assay set-up, facilitates automated read-out and minimizes risks associated with hazardous viruses. Based on this assay system, we screened 7035 small molecule compounds from which we identified 7 compounds with anti-SARS-CoV activity. We demonstrate that the compounds inhibited SARS-CoV replication-dependent GFP expression in the replicon cells and reduced SARS-CoV viral protein accumulation and viral RNA copy number in the replicon cells. In a SARS-CoV plaque reduction assay, these compounds were confirmed to have antiviral activity. The target of one of the hit compounds, C12344, was validated by the generation of resistant replicon cells and the identification of the mutations conferring the resistant phenotype. These compounds should be valuable for developing anti-SARS therapeutic drugs as well as research tools to study the mechanism of SARS-CoV replication.

© 2008 Elsevier B.V. All rights reserved.

1. Introduction

The severe acute respiratory distress syndrome (SARS) emerged at the beginning of 2003 and rapidly spread throughout the world (Drosten et al., 2003; Ksiazek et al., 2003; Peiris et al., 2003; Zhong et al., 2003). Although the disease had disappeared in June 2003, its re-emergence cannot be excluded. The development of vaccines against SARS-CoV may take years. Therefore, the availability of effective antiviral drugs against SARS-CoV may be crucial for the control of future SARS outbreaks.

Severe acute respiratory syndrome is a severe febrile lower respiratory illness caused by a newly identified coronavirus, the SARS coronavirus (SARS-CoV) (Drosten et al., 2003; Ksiazek et al., 2003; Peiris et al., 2003). The SARS-CoV genome encompasses 29,727 nucleotides and the genome organization is similar to that of other coronaviruses. The genome is predicted to contain 14 functional open reading frames (ORFs) (Marra et al., 2003; Rota et al., 2003; Thiel et al., 2003a). SARS-CoV genome expression starts with the

translation of two large replicative polyproteins, pp1a (486 kDa) and pp1ab (790 kDa), which are encoded by the viral replicase gene (21,221 nt) that comprises ORFs 1a and 1b. The remaining twelve ORFs encode the four structural proteins, S, M, N and E, and eight accessory proteins (Thiel et al., 2003a; Ziebuhr, 2004).

SARS-CoV drug discovery requires the development of reliable biological assays. Traditional antiviral assays for coronavirus are based on viral infection of cultured cells, followed by monitoring of compound inhibition of viral replication through observation of cytopathic effects, quantification of viral yields by plaque assay, or measurement of viral RNA by reverse transcription-PCR (Ivens et al., 2005; Wu et al., 2004). The virus can infect many cell types and produces plaques (Hofmann and Pöhlmann, 2004). However, the requirement that infectious virus work be carried out under Biosafety Level 3 conditions makes it more difficult to use live virus assays in high-throughput screening (HTS) to identify antiviral compounds. The low-throughput nature of these assays limits their use for the screening of compound libraries. The availability of reverse genetic systems for many coronavirus (cDNA clones for infectious full-length genomes and for subgenomic replicons) has made it possible to develop novel assays for HTS (Thiel et al., 2003b; Yount et al., 2000, 2003). In principle, a reporter gene such as GFP could be engineered into a full-length virus and into a subgenomic

* Corresponding author. Tel.: +86 20 85224372; fax: +86 20 85227039.

E-mail address: tgfeng@jnu.edu.cn (F. Ge).

¹ These two authors equally contributed to this work.

replicon. Infection or transfection of susceptible cells with such a reporting virus or replicon results in the expression of GFP. The level of GFP fluorescence would reflect the extent of viral replication and could be used to monitor the suppression of viral infection by potential inhibitors (Ge et al., 2007; Hertzog et al., 2004).

A stable BHK cell line replicating SARS-CoV replicons expressing a green fluorescent protein (GFP) gene co-expressed from a polyprotein containing the selectable marker gene, blasticidin-resistant gene (BlaR) has been recently described (Ge et al., 2007). Here we report the utilization of this cell line in a 96-well format high-throughput screen, and report on our initial success in using this assay to identify compounds with antiviral activity from a screen of a library of 7035 compounds. From this screen we have identified seven small molecules that reduced the GFP fluorescence, as well as SARS-CoV protein and RNA synthesis in the SARS-CoV replicon cells. The efficacies of these compounds against SARS-CoV infection in Vero cells have also been measured by a plaque reduction assay (PRA). In addition, the target of one of the hit compounds, C12344, was validated by the generation of resistant replicon cells and the identification of the mutations conferring the drug-resistant phenotype.

2. Materials and methods

2.1. Chemical library

The chemical library screened represents a broad and well-balanced collection of 7035 compounds accumulated over a number of years from a variety of distinct sources. All 7035 of the compounds were provided by the Guangdong Institute of Materia Medica. All compounds were dissolved in dimethyl sulfoxide (DMSO) to 10 mM and transferred to 96-well microtiter plates to assay for antiviral activity. The final compound concentration used in primary screening was 10 μ M, with a final DMSO concentration of 0.5%.

2.2. Cells and media

The SARS-CoV replicon cell line stably expressing a SARS-CoV replicon encoding GFP has been described previously (Ge et al., 2007). These cells were cultured in a 96-well plate in DMEM medium (Gibco) containing 10% fetal calf serum (Gibco) and 10 μ g/ml blasticidin (Invitrogen) and used between passages 25 and 30 to ensure reproducibility.

The baby hamster kidney (BHK)-21 and African green monkey kidney cells (Vero E6) cell lines were purchased from American Type Culture Collection (ATCC) and maintained in Dulbecco's modified Eagle's medium (DMEM; Invitrogen) supplemented with 10% fetal bovine serum (FBS; Invitrogen) at 37 °C in 5% CO₂.

2.3. HTS GFP fluorescence reduction assay and cytotoxicity of the hit compounds

The replicon cells were plated in 96-well Clear-Bottom Plates (Corning Inc., Corning, New York) at 3×10^4 cells/well in DMEM plus 3% FBS and 10 μ g/mL blasticidin. The culture media was removed after a 1-day incubation and replaced by fresh medium without blasticidin. Twenty-four hours later, compounds were added to a final concentration of 10 μ M and 0.5% DMSO using a Biomek NX Robotic liquid handler (Beckman Coulter, Fullerton, CA). The plates were sealed with gas permeable membrane and incubated in a humidified incubator at 37 °C and 5% CO₂. After 2 days, the wells were examined for GFP expression using an argon laser-scanning microscope (Carl Zeiss, Oberkochen, Germany). The microscope settings were excitation at 488 nm and emission at 510 nm and the

fluorescence images of the wells were converted into signal values. Cytotoxicity was measured for primary hit compounds by MTT assay using 96-well plates. Approximately 3×10^4 BHK-21 or Vero E6 cells in 100 μ l of medium were seeded per well in a 96-well plate. After 6 h of incubation, 1 μ l of compound dissolved in DMSO was added to the cells at varied concentrations. After 48 h of incubation when the cells reached 80–90% confluence, 10 μ l of MTT reagent was added to each well and the cells were incubated for another 4 h, after which 100 μ l of detergent reagent was added to each well. The plates were swirled gently and left in the dark at room temperature for 4 h. The absorbance was recorded in a Microtiter plate reader (Molecular Devices Corporation, Sunnyvale, CA) with a 550-nm filter.

2.4. Flow Cytometry Analysis of candidate compounds

Flow Cytometry Analysis was used to determine the IC₅₀ of the candidate compounds. Different concentrations of compounds were added on monolayer of SCR-1 cells in 96-well plates, and an untreated well served as control. Two days later, the cells were analyzed by a Beckman Coulter Epics Altra flow cytometer. Four duplicate tests were performed. Inhibition of reporter gene expression was calculated as reduction of the mean fluorescence intensity (MFI) of GFP-positive cells by setting the MFI of untreated SCR-1 cells as 0% inhibition and the complete down regulation of GFP to background levels as 100% inhibition. The cells were scanned for green fluorescence using a Beckman Coulter Epics Altra flow cytometer. The data collected were analyzed using the WINMDI 2.7 data analysis program (The Scripps Research Institute). The results were expressed as IC₅₀ values defined as the concentration of compound achieving 50% inhibition of the replicon fluorescence signals as compared to the untreated control cells.

2.5. Real-time PCR analysis

Real-time RT-PCR analyses were performed to quantify the copy number of replicon RNA in SCR-1 cells before and after drug treatment. Primers and RT-PCR conditions were used as previously described (Drosten et al., 2003; Ge et al., 2007). Real-time PCR signals were analyzed using the LightCycler software (Roche; version 5.32), and the sizes and uniqueness of PCR products were verified by performing both melting curves and agarose gel electrophoresis. The copy number of replicon RNA was determined by direct comparison with the internal standards. Replicon RNA expression levels are expressed as number of copies/ μ g total RNA. Each datum point represents the average of five replicates in cell culture.

2.6. Detection of SARS-CoV replicon expressed proteins by western blotting

Total cell lysates were harvested from replicon cells or BHK-21 cells in 1 \times SDS sample buffer. The lysates were heated at 70 °C for 10 min in the presence of DTT before electrophoresis on a 10% SDS-PAGE gel, transferred onto polyvinylidene difluoride (PVDF) membranes (Millipore Corporation, Billerica, MA) and then blocked using Tris-buffered saline Tween-20 (TBS-T) buffer containing 5% non-fat milk. Membranes were next hybridized overnight in the cold room using anti-nsp5 (3CL^{pro}) antibody (a kind gift from Dr. Zhang Liang at the Guangzhou Medical College); washed three times in ice cold TBS-T; and then incubated with goat anti-rabbit horseradish peroxidase (HRP)-conjugated antibody (1:2000; Promega) for 1 h. The reaction was detected using the ChemiGlow chemiluminescence reagents (Alpha Innotech, San Leandro, CA). Image spot densitometry was performed on the Alpha Imager (Alpha Innotech). For controls, the blots were stripped and

re-probed anti-actin (Santa Cruz Biotechnology, Santa Cruz, CA) mAbs, which was detected as described above.

2.7. Viral plaque reduction assay

SARS-CoV strain BJ-01 was kindly provided by the Chinese National Institute for Viral Disease Control and Prevention. The degree of protection offered by the test compounds against SARS-CoV infection was measured by plaque reduction assay. Briefly, one hundred plaque forming units (PFU) of SARS-CoV were added to individual wells of 24-well tissue culture plates seeded with a monolayer of Vero cells (1×10^5 cells per well) in DMEM with 1% FBS. After a 1 h incubation, the inocula were removed and the cells were washed with phosphate-buffered saline solution (PBS). One millilitre of overlay (1% low-melting agarose in DMEM with 1% FBS and either lacking test compound or with different concentrations of compounds) was added to each well. After 48 h of incubation at 37 °C in 5% CO₂, the culture medium was removed and the cells in the culture plate were fixed with a 10% formalin solution and stained with crystal violet solution. The plaque number was then counted. The 50% inhibitory concentration (IC₅₀) was defined as the concentration at which the plaque number was reduced to half of that in cells cultured without addition of antiviral drugs. The same experiment was performed three times independently for each drug and the IC₅₀ values were calculated as the average \pm standard deviation (S.D.) of the three experiments. All procedures involving manipulation of live SARS-CoV were carried out in a biological safety level 3 containment laboratory.

2.8. Generation of resistance in replicon cells

To evaluate generation of viral resistance against specific inhibitors, replicon cells were plated in six-well plates at a density of 2×10^5 cells per well and serially passed in the presence of 10 μ g/ml blasticidin and 5 μ M of inhibitor. Fresh media and compounds were added to the monolayer every 3–4 days. Cells were split whenever they reached 70% to 80% confluence. For no compound control cells, little cell death was observed, and a monolayer of the cells was maintained throughout the culture. For cells incubated with blasticidin and inhibitor, most cells died after 2–3 weeks, while small colonies (in the order of 10–20 cells) started to appear, which were expanded for another 2 weeks and were analyzed for the presence of specific resistant mutations in the SARS-CoV nsp5 protease domain.

2.9. Statistical analysis

Statistical analysis was performed using two-tailed Student's *t*-test, and $p < 0.05$ was considered significant. Data were expressed as the mean \pm S.D. of triplicate samples, and reproducibility was confirmed in three separate experiments.

3. Results

3.1. Optimization of the microplate-based fluorescence assay for HTS mode

We have recently described a cell line (SCR-1) that stably expresses a SARS-CoV replicon that encodes a GFP reporter gene and a blasticidin-resistant gene (Fig. 1A). It allows viral replication to be monitored by simply measuring the fluorescence intensity in the cells. To adapt a GFP-expressing replicon cell line (SCR-1) into an HTS assay, we initially determined a linear range of reporting cells for seeding of the 96-well plates. Selection of an appropriate cell number per well is critical because cell density could affect

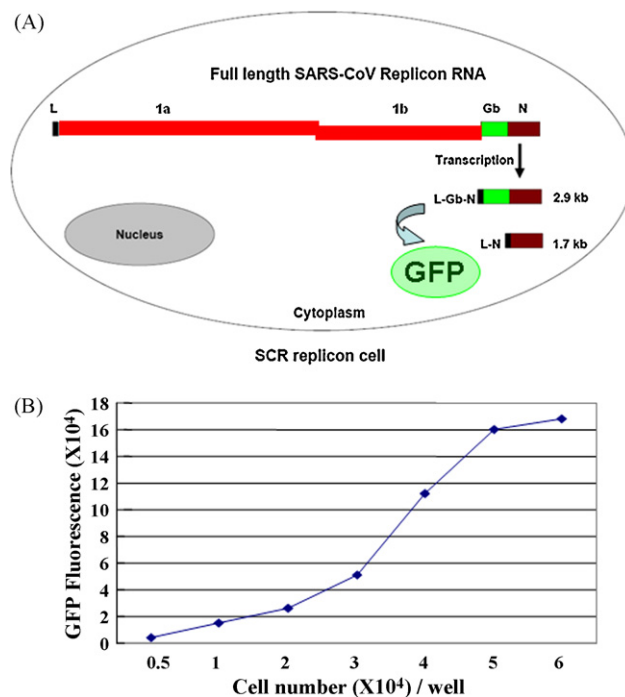


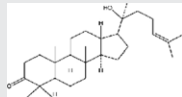
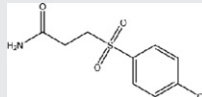
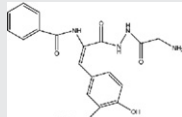
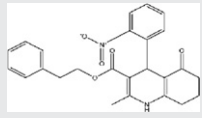
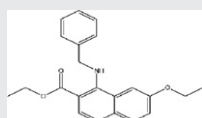
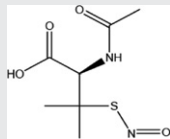
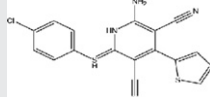
Fig. 1. (A) Schematic representation of the SARS-CoV replicon used for HTS. The subgenomic replicon genomes are depicted with the genes shown as boxes. Gb stands for green fluorescent protein-blasicidin deaminase fusion gene, L stands for leader sequence. Gb gene was inserted between SARS-CoV ORF1b and N gene. (B) Detection of GFP fluorescence in 96-well plates of SCR-1 cells demonstrating the linear relationship between cell number and the intensity of GFP fluorescence.

the replication efficiency of the replicon, and analysis of inhibitors requires quantification of a decrease in the steady-state level of replicon RNA. To examine the effects of cell density, SCR-1 cells were seeded at densities ranging from 5000 to 60,000 cells/well. The fluorescence signal correlated closely with cell number (Fig. 1B). We were able to consistently produced easily measurable fluorescence signals at a density of 30,000 cells/well, so this density was selected for the HTS assay. Furthermore, at this density the cells did not become overly confluent during the assay, a condition in which replicon copy number might be adversely affected (Pietschmann et al., 2001). We next examined the effect of cell passage on fluorescence intensity and showed that the activity was stable for at least 10 passages (data not shown). All HTS assays were performed with cells that were within 5 passages from the original frozen stocks (passage 25–30 from colony selection). The impact of DMSO concentration was also examined; the results revealed that the cells tolerated 0.5% DMSO, but there was a slight decrease in the fluorescence signal when 2% DMSO was used (data not shown). Therefore, in the HTS assay the DMSO concentration was limited to 0.5%. Under this experimental condition, the assay window (GFP fluorescence signal from replicon-bearing cells divided by the background signal from naïve BHK-21 cells) consistently ranged from 1×10^4 to 1×10^5 (data not shown). The results suggest that the replicon-containing cell line could be used in an HTS assay.

3.2. HTS screening to identify SARS-CoV inhibitors

We screened over 7035 compounds in the HTS assay at a single concentration of 10 μ M in single cells. Employing a 50% reduction in fluorescence signal as the criterion for further evaluation approximately 105 compounds were identified (~1.5% hit rate). To eliminate false positives and/or cytotoxic compounds, these compounds were re-evaluated at 10 μ M concentration man-

Table 1
Summary of HTS compounds with activity in SARS-CoV replicon cells^a

Compound ^b	Structure	Chemical name	Replicon (BHK)		SARS-CoV (Vero)	
			IC50 (μM) ^c	CC50 (μM) ^d	IC50 (μM) ^e	CC50 (μM) ^f
C01225		(5R,9S,14R)-dodecahydro-17-((S)-2-hydroxy-6-methylhept-5-en-2-yl)-4,4,8,10-tetramethyl-2Hcyclopenta[a]phenanthren-3(4H,9H,14H)-one	3.1 ± 0.19	>100	7.3 ± 2.09	>100
C03455		3-(4-Chlorobenzenesulfonyl)-propionamide	5.8 ± 0.31	87 ± 5.23	4.5 ± 1.31	>100
C11472		(E)-N'-(2-aminoacetyl)-2-(benzamido)-3-(4-hydroxy-3-methoxyphenyl)acrylohydrazide	3.2 ± 0.37	>100	11.3 ± 2.56	82 ± 4.33
C12344		3-Quinolinecarboxylic acid, 1,4,5,6,7,8-hexahydro-2-methyl-4-(2-nitrophenyl)-5-oxo-, 2-phenylethyl ester	2.0 ± 0.45	>100	8.9 ± 1.17	>100
C26505		4-Benzylamino-6-ethoxy-quinoline-3-carboxylic acid ethylester	2.1 ± 0.09	78 ± 4.87	7.6 ± 1.21	>100
C38477		S-Nitroso-N-acetyl penicillamine	1.4 ± 0.11	58 ± 1.22	3.2 ± 1.97	84 ± 2.96
C47655		2-Amino-6-[(4-chlorophenyl)thio]-4-(2-thienyl)pyridine-3,5-dicarbonitrile	2.1 ± 0.16	>100	6.8 ± 1.87	>100

^a The data represent the averages of three or more independent experiments.

^b The name of the compound corresponds to the catalog number in our compound library.

^c IC50: concentration of the compound that produces 50% decrease in GFP fluorescence. The highest concentration of compounds used in IC50 determination is 100 μM.

^d CC50: concentration of compound that produced 50% decrease in MTT signals. The compounds were tested up to 100 μM. Cytotoxicity was tested in BHK-21 cells.

^e IC50: the concentration at which the plaque number decreased to half of that in cells cultured without addition of antiviral drugs. The reduction in viral titers was determined by plaque assays on Vero cells, as described in Section 2. The highest concentration of compounds used in IC50 determination is 100 μM.

^f CC50: concentration of compound that produced 50% decrease in MTT signals. Cytotoxicity was analyzed in Vero E6 cells.

ually. Duplicate 96-well plates were prepared for side-by-side fluorescence assay and toxicity determination to rule out toxic compounds. Upon completion of these assays, 37 compounds reduced GFP fluorescence less than 50% in this re-test and 61 compounds were toxic to BHK cells. As a result, 7 preliminary candidate compounds were selected for further analysis and triage.

In an attempt to quantify the activity of the 7 remaining candidate compounds, a serial dilution of each compound was prepared and assayed with the SCR-1 cells to determine the IC50 for the fluorescence readout. The dose-response curves for these 7 compounds yielded IC50 values of 1.4–5.8 μM (Table 1) and the variability in the results between triplicate fluorescence wells was low, with no aberrant results evident over the range of drug concentrations tested.

3.3. Confirmation of the SARS-CoV replicon inhibitor compounds

The candidate compounds were next further assessed in secondary assays to ascertain that they inhibited the SARS-CoV

replicon. Firstly, to demonstrate that the compounds can inhibit SARS-CoV replicon RNA replication, we utilized Real-time PCR to analyze the SARS-CoV RNA level in SCR-1 cells treated with the candidate compounds. Fig. 2 shows that compared to the untreated control, replicon RNA levels were significantly reduced after 48 h treatment and the candidate compounds reduced replicon RNA levels in a dose-dependent manner. When the log₁₀ change in replicon RNA copy number was calculated for the assay, these compounds reduced the copy number per μg RNA by approximately 2 log₁₀ at 2.5 μM and 5 log₁₀ at 10 μM, respectively. After 48 h incubation with these compounds, no significant cytotoxicity, as evaluated in an MTT-based cell viability assay, was observed in the replicon cell at a concentration up to 100 μM of these compounds.

Secondly, the anti-SARS-CoV activity of these compounds in replicon cells was also examined at the protein level using Western blot analysis. The specificity of the antibody against the SARS-CoV nsp5 was first confirmed using Western blot analysis, which

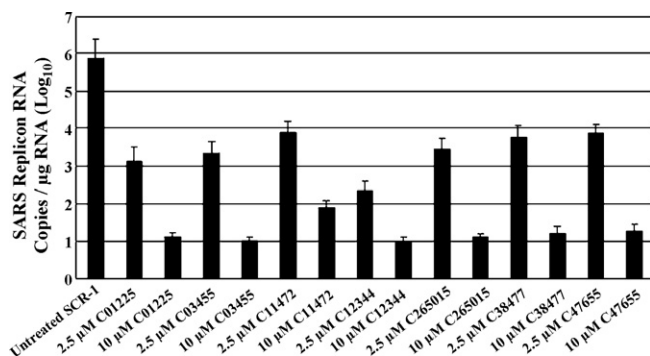


Fig. 2. Quantitative Real-time RT-PCR analysis of compounds treated SARS-CoV replicon cells. Copy number of SARS replicon RNA in SCR-1 cells before and after inhibitor treatments are shown. The inhibitors used are indicated below. Data are the means of five independent experiments. Bar: 95% confidence intervals.

showed that the SARS-CoV proteins were present in the replicon cells but not in the parental BHK-21 cells (Fig. 3A). In the Western blot analysis shown in Fig. 3B, total cell proteins were prepared from SARS-CoV replicon cells treated with the candidate compounds and the viral protein nsp5 was detected with the anti-nsp5 (3CL^{pro}) antibody. The same blots were stripped and probed for beta-actin to show equal loading. As shown in Fig. 3B, all of the compounds had minimal effect on the beta-actin level, which is consistent with the MTT data showing that these compounds are not cytotoxic at the 10 μM concentration used. The Western blot data demonstrate that the tested compounds all reduced SARS-CoV nsp5 protein level in replicon cells after 48 h drug treatment. Dose dependency is also clearly seen with several compounds, e.g. C12344 and C26505 (structures shown in Table 1). However, a few compounds reduced viral protein only at 10 μM, the highest concentration used. Examples include C03455 and C11472 (Table 1). Comparison of these Western blot data with the IC₅₀ data determined with the FACS assay, demonstrated a reasonably good correlation between fluorescence reduction and viral protein reduction. All these data

indicate that the candidate compounds that inhibited SARS-CoV replicon RNA replication also prevented replicon protein synthesis.

Thirdly, these compounds inhibited the SARS-CoV plaque formation in Vero cells in a concentration-dependent manner with IC₅₀ values between 3.2 ± 1.97 and 11.3 ± 2.56 μM (Table 1), demonstrating that the protective effects observed were indeed due to the presence of inhibitors. These results demonstrate that comparable IC₅₀s could be obtained from the replicon assay system and from the authentic SARS-CoV infection assay. Furthermore, the CC₅₀ values of these candidate compounds in Vero cells were determined to be >80 μM (Table 1), indicating that these compounds are not cytotoxic at their effective antiviral concentrations. In summary, the results presented above clearly demonstrate that the replicon assay can be used for HTS of compound libraries.

3.4. Emergence of C12344-resistant variants in replicon cells

Of the 7 preliminary candidate compounds, one of the compounds (designated C12344) displayed potent inhibitory activity with an IC₅₀ of 2.0 μM. The finding is in line with previous reports (Kao et al., 2004a,b). It is reported that C12344 is a specific SARS-CoV 3CL^{pro} inhibitor and can be docked favorably into the active site of SARS-CoV 3CL^{pro} (Kao et al., 2004b). To validate the target of C12344, the chemical-resistant replicon cells were selected and the genetic mutations conferring the resistant phenotype were identified. Briefly, the SARS-CoV replicon cells were plated in six-well plates and in the presence of 10 μg/ml blasticidin and 5 μM of C12344. Small colonies (10–20 cells in size) were observed at 18 days and a total of 59 or 60 large colonies (with 50–100 cells per colony) were recovered in two separate wells at day 25. For cells recovered in the presence of antiviral agents, the nucleotide sequences of the SARS-CoV 3CL^{pro} cDNA were determined after RNA extraction and RT-PCR, as described previously (Ge et al., 2007). Two resistance variations against C12344 were identified to be substitutions of Lys61 with Ile (K61I) and Asn119 with His (N119H). Since these nucleotide changes were not encoded by the original replicon cDNA, they, most likely, have been acquired during repli-

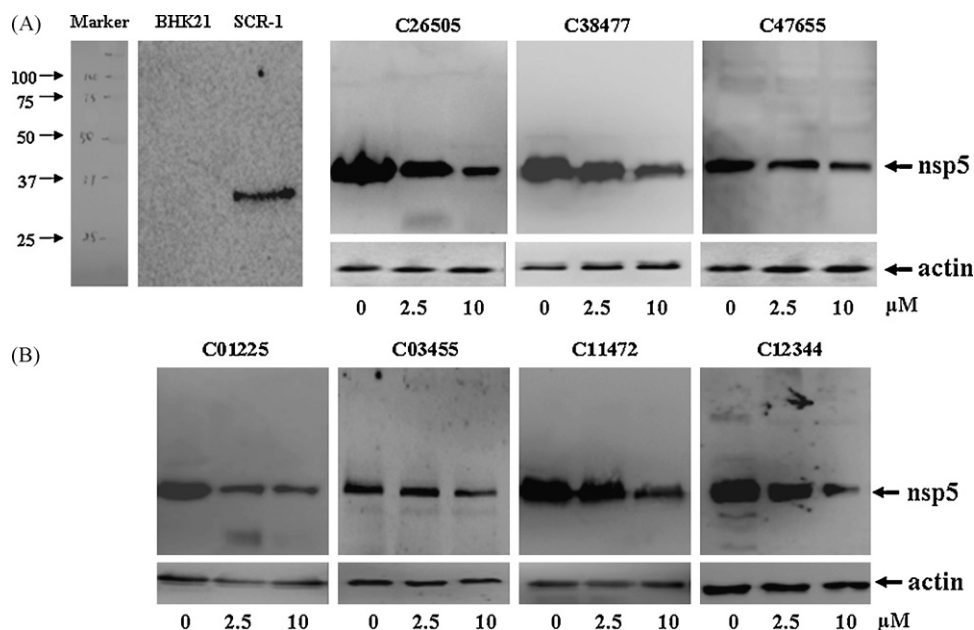


Fig. 3. Western blot analysis of the SARS-CoV protein from compound-treated replicon cells. (A) Specificity of the antibody against SARS-CoV nsp5 in Western blot analysis. Cell lysates from the parental BHK-21 or SCR-1 replicon cells were analyzed by SDS-PAGE, transferred, and probed with specific antibody against nsp5. The molecular weight markers are indicated on the left. (B) Reduction of SARS-CoV proteins in Western blot. Equal amounts of protein from each cell extract were subjected to SDS-PAGE and subsequent Western blot analysis with specific antibodies against nsp5 or actin (bottom).

cation in cell culture and are the marker mutations related to drug resistance.

4. Discussion

An important aspect of drug screening for new viral diseases is the choice of the assay system. The goal of this study was to explore genetic system for the development of HTS assays for SARS-CoV drug discovery. In this report, we describe the development and use of a SARS-CoV replicon-based HTS screen and the discovery of compounds with potential antiviral activity from a library of 7035 compounds. The assay used a preliminary screening concentration of 10 μ M and detected antiviral activity by measuring levels of GFP fluorescence, which was encoded in the SARS-CoV replicon. Preliminary candidate compounds were defined by their ability to reduce GFP fluorescence activity by more than 50%. These preliminary candidates were validated by retesting, and demonstrating absence of cytotoxicity, which would also have reduced GFP fluorescence in the replicon-bearing cells. Activity of this set of hits against SARS-CoV replication was confirmed by demonstrating that the compounds reduced the levels of SARS-CoV RNA and protein in replicon-bearing cells.

Using the replicon assay, we identified 7 compounds that met our criteria of selective inhibition of SARS-CoV RNA and/or protein accumulation. The 7 compounds are presented in Table 1. The finding that C12344 and C01225 showed selective activity against SARS-CoV is in line with previous reports (Kao et al., 2004a; Lai et al., 2006; Wu et al., 2004; Yang et al., 2006). A previous report also found that compounds C26505 and C03455 were active against West Nile virus (Gu et al., 2006). The remaining three compounds are chemically attractive (chemically stable, non-reactive, and easy to synthesize derivatives) and appear to be well suited for further analysis. Most importantly, all these compounds inhibited SARS-CoV viral production in live virus infection assays. All these compounds show a potential for further optimization into potent inhibitors of SARS-CoV and merit detailed characterization regarding mechanism of action. At present, only the target of C12344 has been validated by the generation of resistant replicon cells and the identification of the mutations conferring the drug-resistant phenotype, the mechanisms of action for the remaining six candidate compounds are not known. Whether the compounds are targeting a viral protein or a cellular process that is involved in SARS-CoV replication is not clear. To assess some of these aspects in vitro, we are establishing SARS-CoV 3CL^{pro} and helicase assays to investigate whether the compounds can inhibit these enzymatic activities. At the same time, we are attempting to develop virus resistance to these candidates in order to find out whether a specific viral protein is targeted by their action.

Given the error-prone replication by the viral RNA-dependent RNA polymerase, preexisting variants that are resistant to specific anti-SARS-CoV drugs, such as SARS-CoV 3CL^{pro} inhibitors, could get selected over wild-type SARS-CoV during therapy. We demonstrated that such resistant variations have been selected in vitro against the SARS-CoV 3CL^{pro} specific inhibitor C12433. Therefore, despite the potent anti-SARS-CoV activity of C12433 demonstrated in the replicon cells, the optimal therapy could still involve the combination of C12433 with other antiviral agents. This has been best illustrated with the treatment for HIV, where the combination of three or more drugs of various mechanisms is absolutely necessary to continuously suppress viral replication and the emergence of resistance. In future, we will examine whether the effect of the combination of several drugs was additive or synergistic. Also we are going to investigate whether incubation of the replicon cells with a combination of several drugs would help suppress the emergence of these in vitro resistance variations against C12433.

In conclusion, this report describes a robust screening system for identification of drug candidates selectively active against SARS-CoV. This screening system meets the requirements of a successful high-throughput assay such as minimal manipulation after assay set-up, low sample volume and automated detection of endpoint. This system offers considerable benefits from a first round of screening regarding selectivity, specificity and toxicity of the compound, resulting in an improved data set from an initial screen in comparison with existing assays based on simpler observation such as plaque formation or analysis of CPE. This system, with its ease of handling and good level of safety is well suited to drug discovery against the SARS-CoV, and should be applicable to other emerging high-risk pathogenic viruses. Furthermore, the compounds we have identified may be useful research tools in dissecting the molecular mechanisms of SARS-CoV replication and viral host interaction.

Acknowledgments

We thank Professor Zhang Zirong for providing the compound libraries and setting up the high-throughput screen assay, Dr. Xia Mingzhong for helping the Western blot analysis, Dr. Zhang Jun for helping the Real-time RT-PCR, Dr. Li Xing for Viral plaque reduction assay. This work was supported by the Talents Start-up Foundation of Jinan University (grant 51207040); Program for New Century Excellent Talents in University (grant NCET-07-0376) and the National Natural Science Foundation of China (grant 30400071).

References

- Drosten, C., Günther, S., Preiser, W., van der Werf, S., Brodt, H.R., Becker, S., Rabenau, H., Panning, M., Kolesnikova, L., Fouchier, R.A., Berger, A., Burguière, A.M., Cinatl, J., Eickmann, M., Escriviou, N., Grywna, K., Kramme, S., Manuguerra, J.C., Müller, S., Rickerts, V., Stürmer, M., Vieth, S., Klenk, H.D., Osterhaus, A.D., Schmitz, H., Doerr, H.W., 2003. Identification of a novel coronavirus in patients with severe acute respiratory syndrome. *N. Engl. J. Med.* 348, 1967–1976.
- Ge, F., Luo, Y.H., Liew, P.X., Hung, E., 2007. Derivation of a novel SARS-coronavirus replicon cell line and its application for anti-SARS drug screening. *Virology* 360, 150–158.
- Gu, B.H., Ouzunov, S., Wang, L.G., Mason, P., Bourne, N., Cuconati, A., Block, T.M., 2006. Discovery of small molecule inhibitors of West Nile virus using a high-throughput sub-genomic replicon screen. *Antiviral Res.* 70, 39–50.
- Hertzog, T., Scandella, E., Schelle, B., Ziebuhr, J., Siddell, S.G., Ludewig, B., Thiel, V., 2004. Rapid identification of coronavirus replicase inhibitors using a selectable replicon RNA. *J. Gen. Virol.* 85, 1717–1725.
- Hofmann, H., Pöhlmann, S., 2004. Cellular entry of the SARS coronavirus. *Trends Microbiol.* 12, 466–472.
- Ivens, T., Van den Eynde, C., Van Acker, K., Nijs, E., Dams, G., Bettens, E., Ohagen, A., Pauwels, R., Hertogs, K., 2005. Development of a homogeneous screening assay for automated detection of antiviral agents active against severe acute respiratory syndrome-associated coronavirus. *J. Virol. Methods* 129, 56–63.
- Kao, R.Y., To, A.P., Ng, L.W., Tsui, W.H., Lee, T.S., Tsoi, H.W., Yuen, K.Y., 2004a. Characterization of SARS-CoV main protease and identification of biologically active small molecule inhibitors using a continuous fluorescence-based assay. *FEBS Lett.* 576, 325–330.
- Kao, R.Y., Tsui, W.H., Lee, T.S., Tanner, J.A., Watt, R.M., Huang, J.D., Hu, L., Chen, G., Chen, Z., Zhang, L., He, T., Chan, K.H., Tse, H., To, A.P., Ng, L.W., Wong, B.C., Tsoi, H.W., Yang, D., Ho, D.D., Yuen, K.Y., 2004b. Identification of novel small-molecule inhibitors of severe acute respiratory syndrome-associated coronavirus by chemical genetics. *Chem. Biol.* 11, 1293–1299.
- Ksiazek, T.G., Erdman, D., Goldsmith, C.S., Zaki, S.R., Peret, T., Emery, S., Tong, S., Urbani, C., Comer, J.A., Lim, W., Rollin, P.E., Dowell, S.F., Ling, A.E., Humphrey, C.D., Shieh, W.J., Guarner, J., Paddock, C.D., Rota, P., Fields, B., DeRisi, J., Yang, J.Y., Cox, N., Hughes, J.M., LeDuc, L.W., Bellini, W.J., Anderson, L.J., 2003. A novel coronavirus associated with severe acute respiratory syndrome. *N. Engl. J. Med.* 348, 1953–1966.
- Lai, L.H., Han, X.F., Chen, H., Wei, P., Huang, C.K., Liu, S.Y., Fan, K.Q., Zhou, L., Liu, Z.M., Pei, J.F., Liu, Y., 2006. Quaternary structure, substrate selectivity and inhibitor design for SARS 3C-like proteinase. *Curr. Pharm. Des.* 12, 4555–4564.
- Marra, M.A., Jones, S.J., Astell, C.R., Holt, R.A., Brooks-Wilson, A., Butterfield, Y.S., Khattri, J., Asano, J.K., Barber, S.A., Chan, S.Y., Cloutier, A., Coughlin, S.M., Freeman, D., Girn, N., Griffith, O.L., Leach, S.R., Mayo, M., McDonald, H., Montgomery, S.B., Pandoh, P.K., Petrescu, A.S., Robertson, A.G., Schein, J.E., Siddiqui, A., Smiluis, D.E., Stott, J.M., Yang, G.S., Plummer, F., Andonov, A., Artsob, H., Bastien, N., Bernard, K., Booth, T.F., Bowness, D., Czub, M., Drebot, M., Fernando, L., Flick, R., Garbutt, M., Gray, M., Grolla, A., Jones, S., Feldmann, H., Meyers, A., Kabani, A., Li, Y., Nommund, S., Stroher, U., Tipples, G.A., Tyler, S., Vogrig, R., Ward, D., Watson,

- B., Brunham, R.C., Kraiden, M., Petric, M., Skowronski, D.M., Upton, C., Roper, R.L., 2003. The genome sequence of the SARS-associated coronavirus. *Science* 300, 1399–1404.
- Peiris, J.S.M., Yuen, K.Y., Osterhaus, A.D.M., Stöhr, K., 2003. The severe acute respiratory syndrome. *N. Engl. J. Med.* 349, 2431–2441.
- Pietschmann, T., Lohmann, V., Rutter, G., Kurpanek, K., Bartenschlager, R., 2001. Characterization of cell lines carrying self-replicating hepatitis C virus RNAs. *J. Virol.* 75, 1252–1264.
- Rota, P.A., Oberste, M.S., Monroe, S.S., Nix, W.A., Campagnoli, R., Icenogle, J.P., Penaranda, S., Bankamp, B., Maher, K., Chen, M.H., Tong, S., Tamin, A., Lowe, L., Frace, M., DeRisi, J.L., Chen, Q., Wang, D., Erdman, D.D., Peret, T.C., Burns, C., Ksiazek, T.G., Rollin, P.E., Sanchez, A., Liffick, S., Holloway, B., Limor, J., McCaustland, K., Olsen-Rasmussen, M., Fouchier, R., Günther, S., Osterhaus, A.D., Drosten, C., Pallansch, M.A., Anderson, L.J., Bellini, W.J., 2003. Characterization of a novel coronavirus associated with severe acute respiratory syndrome. *Science* 300, 1394–1399.
- Thiel, V., Ivanov, K.A., Putics, A., Hertzog, T., Schelle, B., Bayer, S., Weissbrich, B., Snijder, E.J., Rabenau, H., Doerr, H.W., Gorbelenya, A.E., Ziebuhr, J., 2003a. Mechanisms and enzymes involved in SARS coronavirus genome expression. *J. Gen. Virol.* 84, 2305–2315.
- Thiel, V., Karl, N., Schelle, B., Disterer, P., Klagge, I., Siddell, S.G., 2003b. Multigene RNA vector based on coronavirus transcription. *J. Virol.* 77, 9790–9798.
- Wu, C.Y., Jan, J.T., Ma, S.H., Kuo, C.J., Juan, H.F., Cheng, Y.S., Hsu, H.H., Huang, H.C., Wu, D., Brik, A., Liang, F.S., Liu, R.S., Fang, J.M., Chen, S.T., Liang, P.H., Wong, C.H., 2004. Small molecules targeting severe acute respiratory syndrome human coronavirus. *Proc. Natl. Acad. Sci. U.S.A.* 101, 10012–10017.
- Yang, H.T., Bartlam, M., Rao, Z.H., 2006. Drug design targeting the main protease, the Achilles' heel of coronaviruses. *Curr. Pharm. Des.* 12, 4573–4590.
- Yount, B., Curtis, K.M., Baric, R.S., 2000. Strategy for systematic assembly of large RNA and DNA genomes: transmissible gastroenteritis virus model. *J. Virol.* 74, 10600–10611.
- Yount, B., Curtis, K.M., Fritz, E.A., Hensley, L.E., Jahrling, P.B., Prentice, E., Denison, M.R., Geisbert, T.W., Baric, R.S., 2003. Reverse genetics with a full-length infectious cDNA of severe acute respiratory syndrome coronavirus. *Proc. Natl. Acad. Sci. U.S.A.* 100, 12995–13000.
- Zhong, N.S., Zheng, B.J., Li, Y.M., Xie, Z.H., Chan, K.H., Li, P.H., Tan, S.Y., Chang, Q., Xie, J.P., Liu, X.Q., Xu, J., Li, D.X., Yuen, K.Y., Peiris, J.S., Guan, Y., 2003. Epidemiology and cause of severe acute respiratory syndrome (SARS) in Guangdong, People's Republic of China, in February. *Lancet* 362, 1353–1358.
- Ziebuhr, J., 2004. Molecular biology of severe acute respiratory syndrome coronavirus. *Curr. Opin. Microbiol.* 7, 412–419.